J. Am. Soc. Mass Spectrom. (2018) 29:1812–1825
DOI: 10.1007/s13361-018-1981-3

FOCUS: APPLICATION OF PHOTONS AND RADICALS FOR MS: RESEARCH ARTICLE

Structural Characterization and Absolute Quantification of Microcystin Peptides Using Collision-Induced and Ultraviolet Photo-Dissociation Tandem Mass Spectrometry

Troy J. Attard,[1,2] Melissa D. Carter,[3] Mengxuan Fang,[1] Rudolph C. Johnson,[3] Gavin E. Reid[1,2,4]

[1]School of Chemistry, The University of Melbourne, Melbourne, VIC, Australia
[2]Bio21 Molecular Science and Biotechnology Institute, The University of Melbourne, Melbourne, VIC, Australia
[3]Division of Laboratory Sciences, National Center for Environmental Health, Centers for Disease Control and Prevention, Atlanta, GA, USA
[4]Department of Biochemistry and Molecular Biology, The University of Melbourne, Melbourne, VIC, Australia

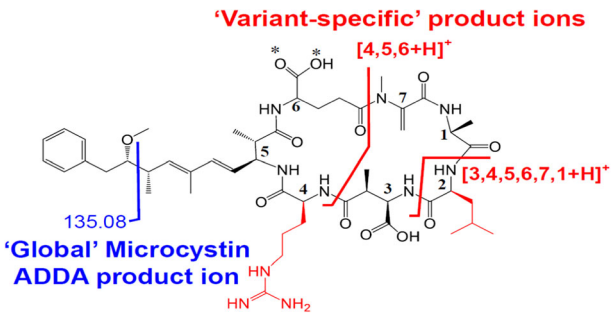

Abstract. Microcystin (MC) peptides produced by cyanobacteria pose a hepatotoxic threat to human health upon ingestion from contaminated drinking water. While rapid MC identification and quantification in contaminated body fluids or tissue samples is important for patient treatment and outcomes, conventional immunoassay-based measurement strategies typically lack the specificity required for unambiguous determination of specific MC variants, whose toxicity can significantly vary depending on their structures. Furthermore, the unambiguous identification and accurate quantitation of MC variants using tandem mass spectrometry (MS/MS)-based methods can be limited due to a current lack of appropriate stable isotope-labeled internal standards. To address these limitations, we have systematically examined here the sequence and charge state dependence to the formation and absolute abundance of both "global" and "variant-specific" product ions from representative MC-LR, MC-YR, MC-RR, and MC-LA peptides, using higher-energy collisional dissociation (HCD)-MS/MS, ion-trap collision-induced dissociation (CID)-MS/MS and CID-MS^3, and 193 nm ultraviolet photodissociation (UPVD)-MS/MS. HCD-MS/MS was found to provide the greatest detection sensitivity for both global and variant-specific product ions in each of the MC variants, except for MC-YR where a variant-specific product uniquely formed via UPVD-MS/MS was observed with the greatest absolute abundance. A simple methodology for the preparation and characterization of ^{18}O-stable isotope-labeled MC reference materials for use as internal standards was also developed. Finally, we have demonstrated the applicability of the methods developed herein for absolute quantification of MC-LR present in human urine samples, using capillary scale liquid chromatography coupled with ultra-high resolution / accurate mass spectrometry and HCD-MS/MS.

Keywords: Microcystin, Tandem mass spectrometry, Ultraviolet photodissociation, Absolute quantitation

Received: 29 March 2018/Revised: 21 April 2018/Accepted: 25 April 2018/Published Online: 29 May 2018

Introduction

Microcystins (MC) are a class of nonribosomal peptides produced as secondary metabolites by a range of cyanobacteria species found in freshwater and brackish

Electronic supplementary material The online version of this article (https://doi.org/10.1007/s13361-018-1981-3) contains supplementary material, which is available to authorized users.

Correspondence to: Gavin Reid; *e-mail:* gavin.reid@unimelb.edu.au

systems worldwide [1]. Algal blooms that arise from a combination of eutrophic conditions and favorable water temperatures can result in MC levels that pose a hepatotoxic threat to aquatic wildlife [2, 3], domestic animals [4, 5], aquaculture enterprises [6, 7], and to human health upon ingestion of contaminated drinking water [8, 9]. The threat to human health is of particular concern, with dose-dependent effects ranging from gastrointestinal distress to severe neurological and liver damage. The possibility of increased risk of cancer as an additional consequence of MC ingestion has also been suggested from several studies reporting a statistical correlation between the incidence of cancer and the occurrence of toxic cyanobacterial populations within the geographical vicinity. However, further evidence is currently limited due to challenges associated with the accurate measurement of exposure to specific MC variants [10–12].

The general structure of MC peptides consist of a cyclic, seven amino acid backbone containing an unusual β-amino acid, (2S,3S,8S,9S,4E,6E)-3-amino-9-methoxy-2,6,8-trimethyl-10-phenyl-4,6-decadienoic acid (ADDA) that is common to MC [13], nodularin [14], and motuporin [15] peptides (Figure 1). Two variable L-amino acids are found at positions 2 and 4 and are represented as a two-letter suffix that forms the basis of MC nomenclature. The remaining residues are considerably more conserved in nature and usually include an *N*-methyldehydroalanine (MDHA), D-Ala, and two acidic residues, D-MeAsp and D-Glu attached to the peptide backbone via their respective β- and γ-side chain carbon atoms. Both proteinogenic and nonproteinogenic substitutions at residues 2 and 4 have been identified in at least 21 known primary analogs [1]; however, methylation or demethylation at those and several other positions provide a major source of structural diversity from which over 90 congeners have been identified to date [16]. Finally, despite the highly conserved nature of the ADDA residue, hydroxyl [17], and acetoxyl [18] variations have also been recorded in addition to the 6(*Z*)-ADDA stereoisomer [19].

The structural elements of MC peptides that are important to toxicity have been identified, particularly through early studies that have examined the relationship between MC variants and their effect on animal cells [20–23]. While the hepatic specificity of MCs results from covalent attachment of protein phosphatases 1 and 2A to the MDHA methylene group (residue 7), the major toxicological determinants have been identified as being due to the presence of a hydrophobic residue at position 2, the free α-carboxylate on the D-Glu residue, and the *E*-stereoisomeric configuration at the C-7 position of ADDA since the absence of any one of these features results in a significant decrease in toxicity [17, 19, 24].

Multiple approaches for the detection of MCs have been used over the past three decades, ranging from toxicological screening to the isolation and identification of specific MC congeners. Protein phosphatase inhibition and immunoassays exhibit high sensitivity toward MCs, but both methods are generally limited by a lack of specificity [25, 26]. More detailed characterization has been provided by liquid chromatography-mass spectrometry (LC-MS)-based approaches, with low-resolution triple-quadrupole analyzers employing selected reaction monitoring (SRM)-collision-induced dissociation (CID)-MS/MS methods, or linear ion trap analyzers, that provide characteristic product ion spectra for a range of MC variants [26–29]. Although not yet widely explored for MC identification and characterization, the more recently developed HCD-MS/MS technique, unique to orbitrap instruments in which fragmentation occurs external to the trap, is of particular interest for MC identification and quantification

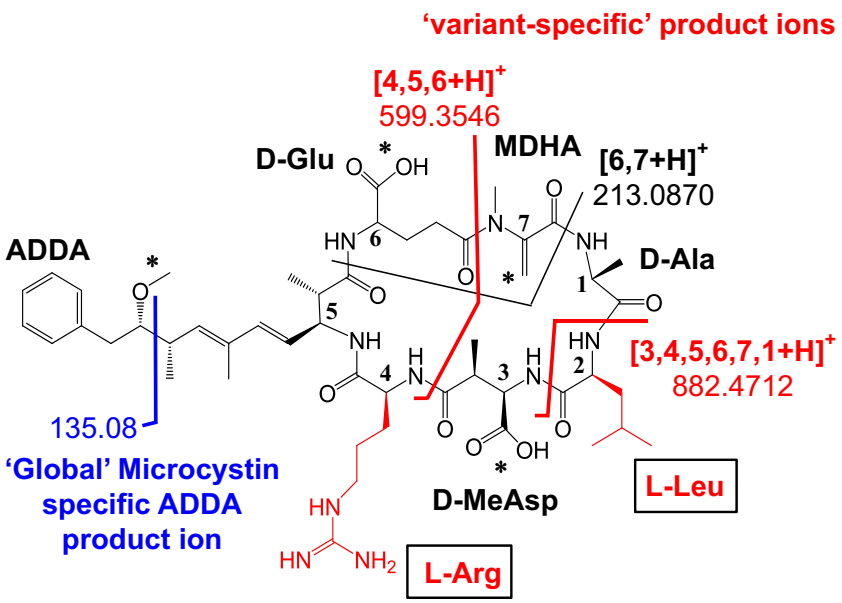

Figure 1. Structure of microcystin-LR, highlighting positions of structural variation in residues 2 and 4 (boxed) and common sites of methylation/demethylation or bioconjugation (asterisk) in microcystin variants. The text highlights the MS/MS cleavage sites and product ion *m/z* values for both global (blue text) and variant-specific (red text) microcystin identification and characterization

from within complex biological matrices. HCD-MS/MS-based parallel reaction monitoring (PRM) techniques [30] provide comparable sensitivity, linearity, dynamic range, and quantitative precision to SRM-CID-MS/MS methods, but with the potential for higher specificity due to acquisition of full MS/MS spectra under high resolution and accurate mass conditions. UVPD is also increasingly employed as an alternative ion activation method for MS/MS-based peptide and protein analysis [31–33], including for proteomics [34] and phosphoproteomics [35], intact proteins [36] and native protein complexes [37], and for the localization of backbone deuteration in peptide hydrogen-deuterium exchange mass spectrometry studies [38]. To date, however, only one publication has described the application of UVPD to cyclic peptides [39], albeit not for the identification and structural characterization of MC peptides.

Finally, traditional methods for the quantification of MCs have relied on absorbance spectroscopy-based immunoassay detection [40, 41] but can lack specificity for individual MC congeners. Furthermore, as stable isotope-containing internal standard reference materials of MC peptides are commercially unavailable, mass spectrometry-based quantitation methods typically rely on the use of analogous molecules such as nodularin as internal standards in complex biological matrices, or employ unlabeled MCs for use in standard addition methods or to generate external calibration curves [42]. However, these methods require multiple analyses or necessitate the use of labor-intensive, matrix-background correction.

The current study addresses these issues through examination of the higher-energy collisional dissociation (HCD)-MS/MS, ion trap CID-MS/MS and CID-MS^3, and 193 nm ultraviolet photodissociation (UPVD)-MS/MS fragmentation behavior of a range of microcystin peptides, along with optimization of the dissociation conditions to provide the greatest detection sensitivity for their unambiguous identification and structural characterization via characterization of both "global" and "variant-specific" product ions. Furthermore, a method for the preparation of ^{18}O-containing reference materials from naturally derived microcystins is also described, as a means to provide internal standards for absolute quantification of MC peptides in complex matrices.

Materials and Methods

Materials

MC-LR, MC-YR, MC-RR, and MC-LA peptides (> 90% purity) were purchased from Boc Sciences (New York, USA). Note that MCs are toxic substances that may be harmful if inhaled or absorbed through the skin or fatal if ingested. Thus, these substances should be dispensed in a fume hood and using appropriate personal protective equipment. All solvents used were of UV spectroscopic grade or higher. Trifluoroacetic acid (TFA, 99%) was obtained from Auspep (Tullamarine, Australia). Formic acid (FA, 99%) was from Ajax Chemicals (Taren Point, Australia).

Preparation of Microcystin Peptide Standard Solutions

MC-LR was prepared at a nominal concentration of 1 μg/μL in methanol based on the quantity indicated by the supplier. Solutions of the remaining MC-YR, MC-RR, and MC-LA peptides were normalized to this concentration to ensure uniformity, based on their relative UV absorbance at 214 nm during RP-HPLC. RP-HPLC was performed using an Agilent 1200 series HPLC (Santa Clara, CA) equipped with a UV detector (model G1365B) and a Grace VisionHT C18 2.1 × 50 mm, 3 μm column. All peptides were dissolved in 2% MeCN/0.1% FA and centrifuged prior to loading. Peptide separation was achieved using a two-step linear acetonitrile gradient from 2 to 25% B in 5 min and 25–60% B in 35 min (buffer A, 0.1% TFA; buffer B, 95% MeCN/0.1% TFA) at a flow rate of 0.25 mL/min.

Capillary LC-ESI-MS and HCD-MS/MS

Analysis was performed by capillary LC-nESI-MS and HCD-MS/MS using an Agilent 1200 Infinity Binary LC System (Santa Clara, CA) coupled to a Thermo Scientific Q Exactive Plus Orbitrap mass spectrometer (Breman, Germany). MC peptides were prepared at various concentrations in 2% MeCN/0.1% FA, then 8 μL loaded onto a Magic AQ C18, 3 μm, 200 Å, 25 × 0.15 mm IntegraFrit Sample Trap Column (Bruker, Billerica, MA) for 5 min at a flow rate at 2 μL/min, followed by elution and separation using a Magic AQ C18, 3 μm, 200 Å, 105 × 0.15 mm PicoChip Column (Bruker, Billerica, MA) using a two-step linear acetonitrile gradient from 2 to 25% B in 5 min and 25–60% B in 35 min (buffer A, 0.1% FA; buffer B, 95% MeCN/0.1% FA) at a flow rate of 0.8 μL/min. Full MS scans were acquired at *m*/*z* 300–2000 with a spray voltage maintained at 2.7 kV, an S-lens setting of 60%, and the ion transfer tube set at 300 °C. Data was recorded at a mass resolving power of 70,000. The maximum injection time was set at 100 ms with an AGC target value of 1.0×10^6. HCD-MS/MS scans were obtained at a resolution of 17,500 with an AGC target value of 1.0×10^6 and an isolation window of 0.8. Evaluation of Normalized Collision Energies (NCSs) within the range of 10–50%, for the optimized identification of both global and variant-specific MC product ions was performed by energy resolved HCD-MS/MS of each peptide, using repeated injections.

Ion Trap CID-MS/MS and MS^n

Linear ion trap ESI-CID-MS/MS and ESI-CID-MS^n experiments were conducted on a Thermo hybrid linear quadrupole Fourier transform-ion cyclotron resonance (LTQ FT-ICR) mass spectrometer (Breman, Germany) operating in positive ionization mode. Each MC peptide was prepared in 50% MeCN/0.1% FA and injected by direct infusion. The spray voltage was maintained at 1.45 kV, while the capillary voltage and temperature was 9 V and 200 °C, respectively. Full-scan mass spectra were acquired over an *m*/z range from 100 to

1100. CID-MS/MS and CID-MS^3 experiments were performed on monoisotopically isolated precursor ions using Q values of 0.25 for singly charged precursor ions and 0.17 for doubly charged precursor ions.

193 nm UPVD-MS/MS

193 nm UVPD MS/MS was performed on a custom-modified Thermo Scientific Q Exactive Orbitrap mass spectrometer using a Coherent ExciStar XS ArF excimer laser (Santa Clara, CA), as previously described by Ryan et al. [43]. MC peptides were introduced to the mass spectrometer via nanoESI (nESI) using an Advion Triversa Nanomate (Advion, Ithaca, NY). Precursor ions were isolated using an isolation window of ± 0.5 *m/z*. The AGC target was maintained at 1×10^6 and the maximum ion injection time was set to 500 ms. The laser power and number of laser pulses for UVPD-MS/MS of each peptide were optimized for formation of the most abundant global or variant-specific product ion, during which the HCD collision energy was set to 1 eV. Control over the ion trapping time, and the HCD collision energy (i.e., below the default value of 10% NCE), was achieved using custom software patches within the mass spectrometer control software. UVPD-MS/MS spectra were acquired in the Orbitrap mass analyzer using a mass resolving power of 70,000 (at *m/z* 400).

Preparation of $^{18}O_2$-Containing Microcystin Peptides and Characterization by Capillary LC-ESI-MS/MS

MC-LR, MC-RR, MC-LA (400 μg), and MC-YR (80 μg) were individually dissolved at 1.25 μg/μL in 5% TFA/$H_2{}^{18}O$ (97 at.%), then extensively sonicated, vortexed, and allowed to sit at room temperature. Progress of the reaction was monitored at different time points by centrifugation of the reaction mixture followed by removal of 1 μL, which was diluted with 2% MeCN/0.1% FA then analyzed by capillary LC-nESI-MS as outlined above. Following satisfactory $^{18}O_2$ incorporation (after 48 h), 4 μL aliquots from the reaction mixture were immediately dispensed into 500 μL Eppendorf tubes and evaporated to dryness by centrifugation under reduced pressure. Dried aliquots were stored at − 80 °C. A dried aliquot from each of the four reaction products was then dissolved in 2% MeCN/0.1% FA using sonication and vortexing, then analyzed by capillary LC-nESI-MS/MS immediately following their preparation, or after 24 h at room temperature to determine the extent of any ^{16}O-back exchange.

Identification and Absolute Quantitation of Microcystin-LR in Human Urine

A 1-mg/mL stock solution of MC-LR in methanol was diluted, using urine from a healthy volunteer as the diluent, to a final concentration of 1 μg/L. A Nanosep® 3K Omega Centrifugal Device (Pall, Melbourne, Australia) was conditioned with 0.08 N NaOH, washed with MilliQ then 500 μL of the MC-LR-spiked urine sample was centrifuged at 3000 rpm until half of the volume remained. The filtrate was acidified with formic acid (5 μL) to pH 2.1 then the entire filtrate volume was extracted through an Oasis HLB 10 mg Extraction Cartridge (Waters Australia, Rydalmere, NSW) using 95% MeCN/0.1% FA as the eluent (5 × 80 μL). The eluent was then evaporated by centrifugation under reduced pressure and the resultant dried sample dissolved in 1 mL of 2% MeCN/0.1% FA; 100 μL of this solution was diluted with 2% MeCN/0.1% FA, then 8 μL was analyzed by capillary LC-nESI-MS and HCD-MS/MS according to the procedure outlined above.

Microcystin MS/MS Fragmentation Nomenclature

In the absence of a universally accepted nomenclature system for cyclic peptide fragmentation, or software for their automated assignments, MC product ions resulting from amide bond cleavages have been manually labeled according to the residues that each product ion contains, along with the molecular weight or molecular formula of any additional fragments within the parenthesis.

Results and Discussion

Identification, Characterization, and Detection Sensitivity Optimization of Microcystin Peptides by Capillary LC-ESI-MS and HCD-MS/MS

Prior to evaluation and optimization of MS/MS fragmentation conditions, the chromatographic and electrospray ionization behavior of four commercially-available microcystin variants, MC-LR, MC-YR, MC-RR, and MC-LA were determined. An equimolar mixture containing the four MC peptide standards was prepared and confirmed by RP-HPLC using UV detection (Supplementary Fig. S1a). This mixture was then analyzed by capillary LC-nESI-MS which revealed significant differences in their ionization potentials across almost two orders of magnitude (Supplementary Fig. S1b), and charge-state distributions (insets to Figure 2a and Supplementary Figs. S2a, S3a, and S4a), correlating with the basicity of the peptide side chains in the order RR > YR ≈ LR >> LA.

Next, the HCD-MS/MS fragmentation characteristics of each of the observed charge states from the four MC variants were examined. Two types of product ions, along with the accurate mass of the precursor, are important for unambiguous identification of an unknown MC congener. The first are those formed from a common structural feature of MC peptides, that serves as a global identifier under a variety of fragmentation conditions. The second type is variant specific and includes only one of the variable residues at position 2 or 4 within the cyclic peptide sequence. The latter category is particularly important in view of the potential for each of these residues to be positionally isomeric in a naturally occurring sequence, the result of which is two variants of identical *m/z*, such as the case for MC-LR/RL and MC-YR/RY [44], particularly for those exhibiting similar chromatographic retention behaviors.

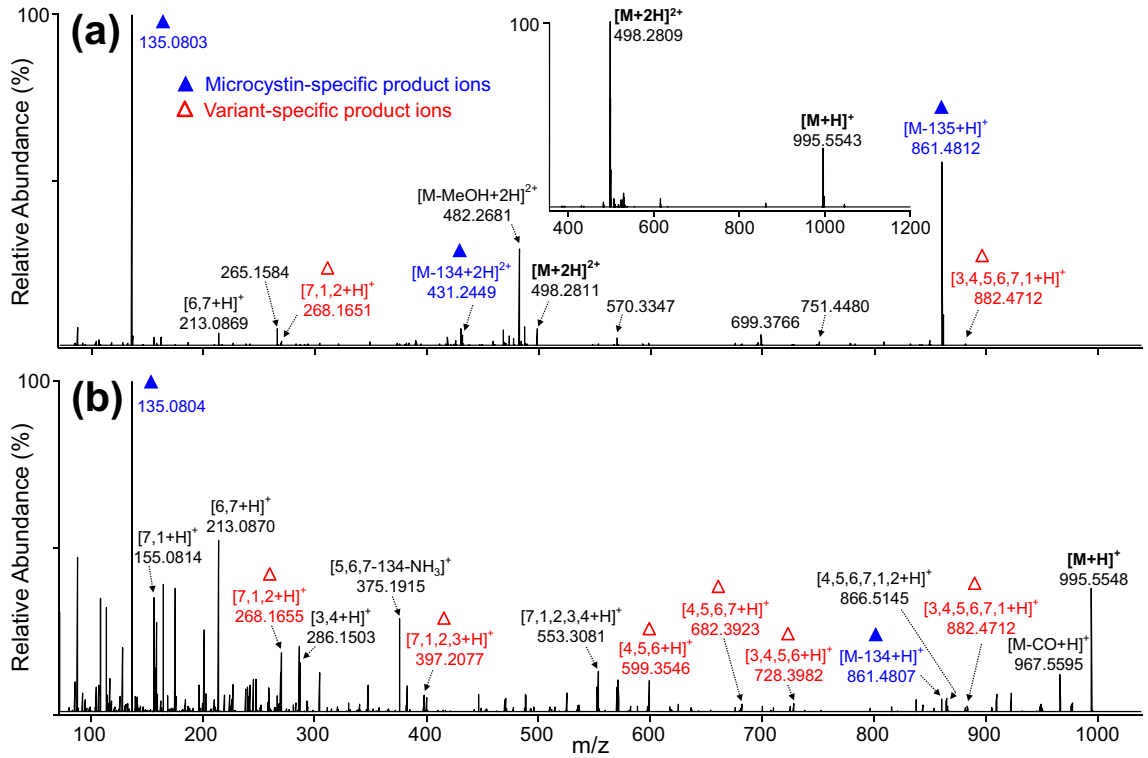

Figure 2. Representative HCD-MS/MS spectra of (**a**) the $[M+2H]^{2+}$ ion (14% NCE) and (**b**) the $[M+H]^{+}$ ion (34% NCE) of microcystin-LR. The ESI-MS spectrum is shown in the inset of (**a**). Global microcystin-specific product ions are indicated by a ▲; variant-specific product ions are indicated by △

A representative HCD-MS/MS product ion spectrum for the $[M+2H]^{2+}$ precursor ion of the MC-LR variant (Figure 2a) is dominated by a product ion at *m/z* 135.08 [Ph-CH_2-$CH(OMe)^{+}$], and its corresponding neutral loss at *m/z* 861.48, characteristic of cleavage occurring within the ADDA side chain (labeled in blue text, and shown in Figure 1). The *m/z* 135.08 product ion has previously been described in the literature as a major product generated under collisional activation conditions, and serves as a global product ion for MC-specific identification due to the presence of this amino acid in all MC variants [27]. This product was also prevalent in the spectrum acquired from the $[M+H]^{+}$ precursor ion (a representative spectrum is shown in Figure 2b), albeit at lower relative abundance. In addition, several variant-specific MC-LR product ions containing either residue 2 or 4 (e.g., $[3,4,5,6,7,1+H]^{+}$, $[4,5,6+H]^{+}$, $[7,1,2,3+H]^{+}$, and $[7,1,2+H]^{+}$ labeled in red text—also see Figure 1) were also observed in either or both of the doubly and singly charged precursor ions. Note that while several other product ions (e.g., $[6,7+H]^{+}$, $[7,1+H]^{+}$, and $[5,6,7\text{-}134\text{-}NH_3+H]^{+}$ in Figure 2b) were observed with greater relative abundances, only the variant-specific product ions provide the required structural information for differentiating this MC-LR variant from other possible isomers. In order to optimize the detection sensitivity for the global and variant-specific product ions, MS/MS spectra were acquired under a range of HCD normalized collision energies, to determine the conditions that give rise to each of these products at their maximum absolute abundances. The results are summarized in Table 1. HCD-MS/MS of the MC-YR peptide resulted in almost identical product ion spectra to those observed for MC-LR, indicating that substitution of leucine for tyrosine in position 2 has little effect on the overall fragmentation behavior (Supplementary Fig. S2). For both peptides, the optimized absolute abundance of the global *m/z* 135.08 product ion was observed to be highest for the doubly-protonated precursors. However, the most abundant variant-specific $[4,5,6+H]^{+}$ product ion was observed from dissociation of the singly protonated precursors (up to twofold higher absolute abundance than the most abundant variant-specific $[3,4,5,6,7,1+H]^{+}$ product ion from the doubly protonated precursors) (Table 1), despite the significantly lower relative abundance of the singly protonated precursor ions.

HCD-MS/MS of the MC-RR precursor ions yielded spectra that were overall similar to those from the MC-LR and MC-YR peptides (Supplementary Fig. S3). While the global ADDA side chain product at *m/z* 135.08 was again observed as the base peak in both cases, and was highest in absolute abundance from the doubly protonated precursor ion, the doubly protonated precursor was observed to provide a variant-specific product ion (i.e., $[7,1,2,3+H]^{+}$) with almost two orders of magnitude greater absolute abundance compared to the $[4,5,6+H]^{+}$ ion from the singly-protonated precursor (Table 1). This is rationalized as being due to the dominance of the doubly charged precursor ion for this peptide owing to the presence of the additional basic Arginine residue. Finally, HCD-MS/MS of the MC-LA peptide from its singly-protonated precursor ion

Table 1. Optimized NCEs for identification of "global" and "variant-specific" microcystin product ions

Product	Optimum normalized collision energy (%)							
	MC-LR		MC-YR		MC-RR		MC-LA	
	$[M+2H]^{2+}$	$[M+H]^{+}$	$[M+2H]^{2+}$	$[M+H]^{+}$	$[M+2H]^{2+}$	$[M+H]^{+}$	$[M+2H]^{2+}$	$[M+H]^{+}$
$[3,4,5,6,7,1+H]^{+}$	22 882.4701 2.3 E5 886.4784	30 882.4729 5.31 E4 886.4808	22 882.4702 2.6 E5 886.4778	28 882.4704 4.76 E4 886.4790	28 882.4734 6.08 E4 886.4795	28 882.4718 1.62 E4 886.4773	–	18 797.4062 2.92 E4 –
$[3,4,5,6+H]^{+}$	18 728.3982 6.49 E4 732.4060	30 728.3984 7.78 E4 732.4061	20 728.3965 8.04 E4 732.4020	28 728.3951 9.22 E4 732.4057	28 728.4007 3.33 E5 732.4059	30 728.3978 6.04 E4 732.4045	–	16 643.3347 3.24 E4 –
$[4,5,6,7+H]^{+}$	–	30 682.3904 5.74 E4 686.3980	–	28 682.3923 9.48 E4 686.4109	28 682.3895 3.72 E5 686.3990	34 682.3894 8.56 E3 686.3992	–	–
$[4,5,6+H]^{+}$	30 599.3534 3.89 E4 603.3646	*30* *599.3551* *3.1 E5* *603.3637*	28 599.3551 6.3 E4 –	*28* *599.3545* *5.12 E5* *603.3651*	28 599.3555 7.65 E5 603.3606	32 599.3547 6.49 E4 603.3633	–	20 514.2912 1.62 E5 518.3022
$[5,6,7,1,2–134\text{-}NH_3]^{+}$	–	28 559.3123 2.32 E4 563.3204	–	28 609.2925 2.93 E4 613.3004	–	28 602.3265 8.20 E3 606.3383	–	*16* *559.3132* *1.12 E7* *563.3196*
$[7,1,2,3+H]^{+}$	34 397.2103 3.97 E4	32 397.2076 1.0 E5	34 447.1869 4.84 E4	30 447.1868 1.29 E5	*36* *440.2256* *4.66 E6*	34 440.2255 5.68 E4	–	26 397.2078 6.89 E6
$[7,1,2+H]^{+}$	– 16 268.1654 1.68 E5	– 32 268.1655 2.09 E5	– 16 318.1446 1.31 E5	– 32 318.1446 2.5 E5	– 40 311.1826 2.18 E6	– 38 311.1821 2.83 E4	–	– *26* *268.1655* *1.12 E7*
$[M\text{-}135]^{+}$ or $[M\text{-}134]^{+}$	– 12 861.4816 9.95 E6 865.4883	– 30 861.4811 1.6 E5 865.5029	– 12 911.4601 1.48 E7 915.4669	– 28 911.4600 2.89 E5 915.4806	– 26 904.4992 4.35 E6 908.5075	– –	– –	– 12 *776.4180* *5.42 E7* *780.4263*
m/z 135	*14* *135.0803* *1.67 E7* –	48 135.0803 3.25 E6 –	*12* *135.0804* *2.29 E7* –	46 135.0804 4.83 E6 –	*36* *135.0805* *9.91 E7* –	50 135.0806 6.51 E5 –	–	40 135.0805 4.37 E7 –

Values set in italics are the most abundant products from either charge state, for the global (blue) and variant-specific (red) product ions. The top value in each row represents the optimal NCE value; the second value is the observed product ion *m/z*; the third value is the absolute intensity of the product ion, the fourth value (where applicable) is the observed *m/z* of the $^{18}O_2$-exchanged peptide product ion

also yielded the global ADDA fragment at *m/z* 135.08 as the base peak signal, along with various variant-specific product ions with significant relative abundances (Supplementary Fig. S4). The low abundance of the doubly charged precursor for the MC-LA peptide dictated that all fragmentation information was obtained from the $[M+H]^{+}$ ion, for which the $[7,1,2+H]^{+}$ product was found to have the highest optimized absolute abundance (Table 1). In general, fragmentation of the MC-LA peptide required considerably lower collision energy than the other peptides, consistent with its increased proton mobility in the absence of a basic Arginine residue [45].

Microcystin Analysis by Linear Ion Trap MS/MS and MS^3

Having optimized the HCD-MS/MS parameters, the fragmentation behavior of the MC peptides was also explored under linear ion trap CID conditions, in order to determine if any further possible signal enhancement for detection of variant-specific product ions would be obtained using this subtly different ion activation process. CID-MS/MS of the $[M+2H]^{2+}$ precursor ion resulted in a dominant non-structurally diagnostic loss of methanol at *m/z* 482.3, along with the global ADDA diagnostic product at *m/z* 135.08, and products formed via neutral or charged losses of the

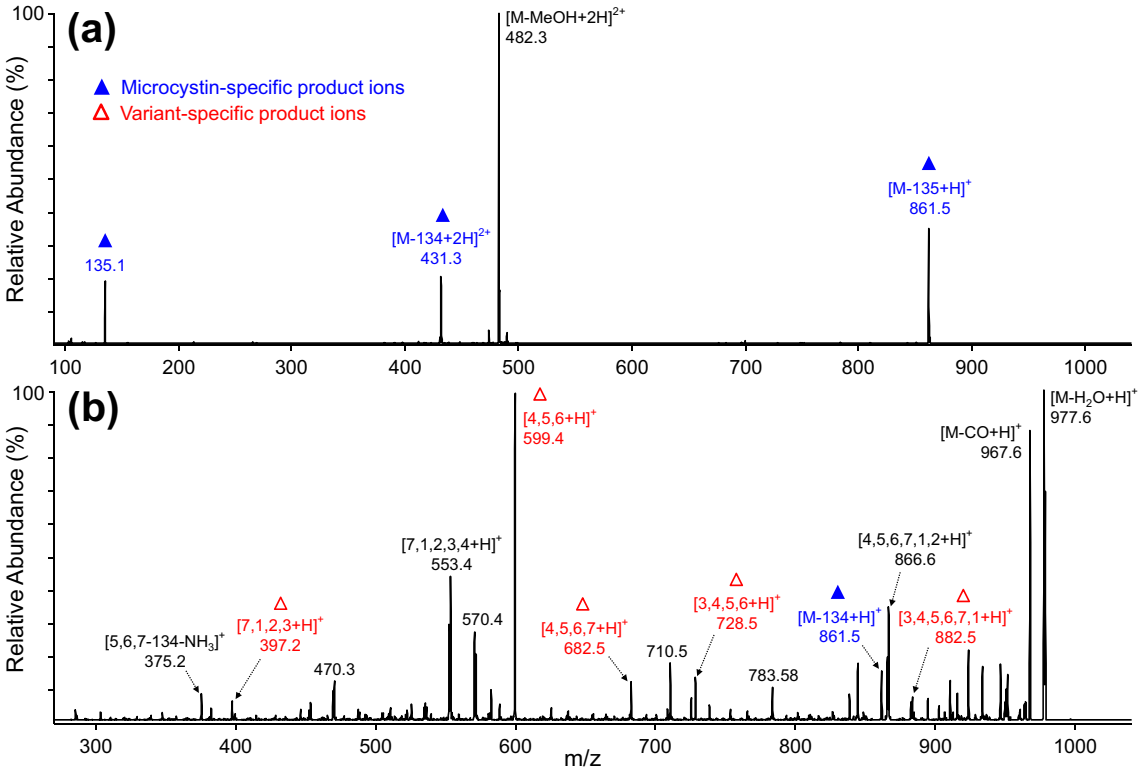

Figure 3. Ion trap CID-MS/MS spectra of (**a**) the $[M+2H]^{2+}$ ion and (**b**) the $[M+H]^{+}$ ion of microcystin-LR. Global microcystin-specific product ions are indicated by ▲; variant-specific product ions are indicated by △

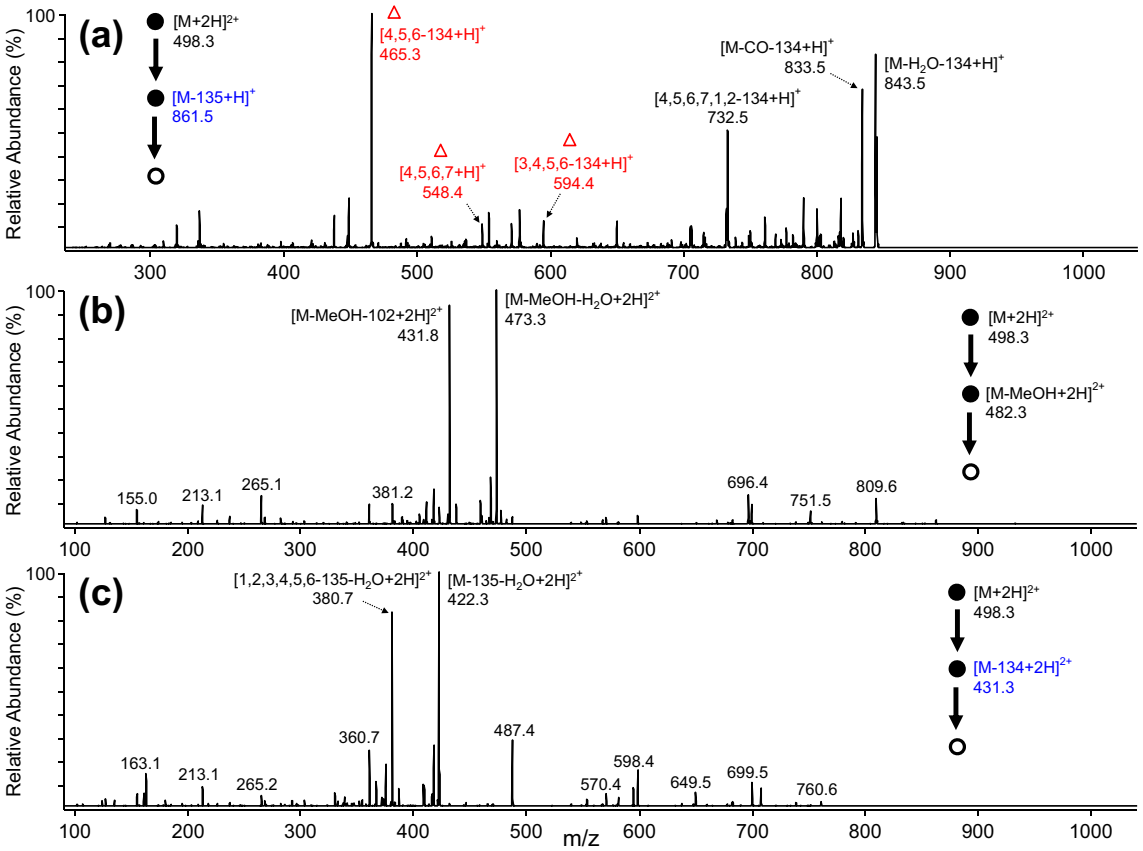

Figure 4. Ion trap CID-MS^3 product spectra of (**a**) the $[M-135+H]^{+}$ ion, (**b**) $[M-MeOH+2H]^{2+}$ ion and (**c**) $[M-134+2H]^{2+}$ ion from the $[M+2H]^{2+}$ precursor ions of microcystin-LR in Figure 3a. Variant-specific product ions are indicated by △

ADDA side chain at *m/z* 431.3 and 861.5, respectively (Figure 3a). Due to the overwhelming dominance of these fragmentation pathways, essentially no variant-specific product ions were observed from this spectrum. However, CID-MS^3 of the *m/z* 482.3, 431.3, and 861.5 ions from Figure 3a (Figure 4a–c, respectively) yielded significantly abundant structurally diagnostic variant-specific product ions (e.g., $[4,5,6\text{-}134+H]^+$) only for the *m/z* 861.5 ion, albeit with a similar absolute abundance to the equivalent $[4,5,6+H]^+$ product ion obtained by CID-MS/MS of the singly protonated MC-LR precursor in Figure 3b (see below). This product ion derived from MS/MS of the MC-LR $[M+H]^+$ precursor was the variant-specific product with the highest absolute abundance, similar to that for HCD-MS/MS, but observation of the ADDA fragment ion was excluded due to the low mass cutoff of the instrument (Figure 3a). Analyses of the MC-YR, MC-RR, and MC-LA peptides also gave similar results (data not shown). These results are consistent with several previous studies that have employed linear ion trap ESI-MS and CID-MS^n for the characterization of MC peptides [27, 46, 47]. However, as no gain in either absolute sensitivity or structural information was provided by using CID-MS/MS or CID-MS^3 compared to HCD-MS/MS, this approach provides no benefit for use in the identification of MC peptides at low concentrations in complex mixtures, particularly when performed on stand-alone ion traps where high resolution and accurate mass analysis is not available.

Microcystin Analysis by 193 nm UVPD-MS/MS

193 nm UVPD-MS/MS of the singly and doubly protonated precursor ions of the MC-LR and MC-RR peptides, the doubly protonated precursor ion of the MC-YR peptide, and the singly protonated precursor ion of the MC-LA peptide, each yielded spectra that were qualitatively similar to that observed by HCD-MS/MS, showing predominantly b- and y-type product ions, albeit with subtle differences in their relative ion abundances (Supplementary Fig. S5, S6, S7, and S8). This is consistent with results from recent literature reports comparing the UVPD- and HCD-MS/MS of linear peptides on a "proteome-wide" scale [31]. However, the absolute abundances of both the UVPD-derived global product ion at *m/z* 135.08 (or its neutral loss $[M\text{-}134+H]^+$ product ion) and the variant-specific product ions, for these peptides, were found to be only approximately half that compared with HCD. This is likely due to the inability to limit secondary photodissociation of these product ions when multiple laser pulses are used to efficiently dissociate the intact precursor ion using the current configuration for UVPD in our custom modified Q Exactive mass spectrometer.

In contrast, UPVD-MS/MS of the singly protonated precursor ion of the MC-YR peptide gave rise to a series of abundant and unique variant-specific product ions formed by neutral loss of the tyrosine side chain (C_7H_8O, *m/z* 803.4053) at residue 2, along with further sequential losses of CO_2 and CONH (*m/z* 759.4153 and 716.4094, respectively), after initial loss of the ADDA side chain (Figure 5). These ions are likely formed due to direct absorption of the 193-nm photons at the aromatic tyrosine residue, leading to preferential cleavage via a charge remote fragmentation pathway due to the "nonmobile" condition of the singly protonated peptide. Notably, the *m/z* 803.4053 and 759.4153 ions were observed with an absolute abundance approximately twice that of the most abundant variant-specific $[4,5,6+H]^+$ product ion observed by HCD, indicating that the use of UPVD-MS/MS would provide a twofold increase in the limit of detection for this MC variant. These data, albeit preliminary and requiring further optimization of the mass spectrometry hardware and data acquisition conditions for more efficient photodissociation, are indicative of the potential utility for UVPD ion activation methods to provide comparable or increased structural information for certain MC peptides.

Development of ^{18}O-Stable Isotope-Labeled Microcystin Reference Materials for Use as Internal Standards

The quantification of microcystins in contaminated biological fluids or tissue ideally requires stable-isotope containing standards that can be added directly to the matrix under investigation, thereby providing a direct comparative measurement of the concentrations of the endogenous material. Several approaches for isotope incorporation are available, including synthetic, conjugative or by exchange reaction with the intact molecule. While the synthetic route involves a straightforward coupling of ^{13}C- or ^{14}N-containing amino acids, a major difficulty lies in preparation of the ADDA amino acid which contains four chiral centers, representing a significant synthetic undertaking [48, 49]. Thus, chemical synthesis methodologies for MC standards are time and economically impractical since the measurement of endogenous MC congeners would require the separate synthesis of each variant. A simpler method was therefore first examined in which a labeled molecule was conjugated to the intact MC peptide. Based on established methods for Michael addition of thiols to the MDHA methylene group of MCs [25, 44], we examined the utility of this approach to incorporate various alkyl amines into MC-LR, using only water as the solvent [50]. Unfortunately, while high reaction efficiencies were observed, LC-MS/MS analysis of reaction products from the conjugation of ethanolamine, 3-aminopropanol or *n*-butylamine to MC-LR showed that the major transition involved β-elimination of the conjugated side chain, which effectively suppressed the detection sensitivity of the isomer-specific product ions (data not shown). In view of this shortcoming, a more convenient, universally applicable approach was sought. Recent literature reports have described acid-catalyzed ^{18}O-exchange from $H_2{}^{18}O$ into intact linear peptides under a variety of conditions [51–53]. Using ^{18}O as an isotopic tag provides a maximum of four possible positions for ^{18}O exchange within the typical MC structure. Hydrochloric acid has been identified as the preferred catalyst on the basis of reaction rate, volatility and the absence of exchangeable ^{16}O atoms that would lead to contamination of the exchange mixture with $H_2{}^{16}O$ [51]. Following the preparation of a saturated $HCl/H_2{}^{18}O$ (97 at.%) solution according to a literature procedure [51], treatment of the MC-LR peptide resulted in complete degradation of the starting material within 6 h, with none of the desired product detected by

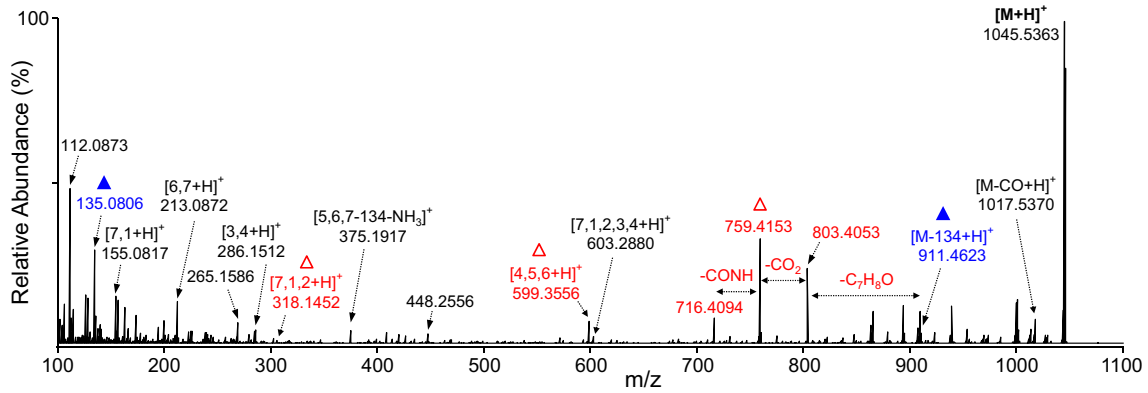

Figure 5. 193 nm UVPD-MS/MS spectra of the $[M+H]^+$ ion (700 V, 20 laser pulses) of microcystin-YR. Global microcystin-specific product ions are indicated by ▲; variant-specific product ions are indicated by △

LC-MS (data not shown). As an alternative therefore, TFA was considered a milder acid catalyst. Although studies describing TFA concentrations above 20% (*v*/*v*) report a significant peptide hydrolysis and a reduced rate of ^{18}O exchange, it was envisaged that lower concentrations with longer reaction times would provide higher purity products [51].

MC-LR samples were treated with solutions containing $H_2{}^{18}O$ (97 at.%) and TFA at either 2.5 or 5% (*v*/*v*) concentrations and monitored by LC-MS at 24, 48, 72, and 96 h time points, at room temperature. As shown in Table 2, the ^{18}O-exchange reaction proceeded smoothly at both concentrations, albeit with a considerable decline in isotopic exchange rate following the incorporation of two ^{18}O atoms (*m/z* 999.6 $[M+H+{}^{18}O_2]^+$). The use of heterogeneous acid mixtures such as 2.5% TFA/9% HCl/$H_2{}^{18}O$ (97 at.%), or heating to 50 °C, resulted in a shift in isotopic distribution toward the $^{18}O_3$ (*m/z* 1001.6 $[M+{}^{18}O_3+H]^+$) and $^{18}O_4$ (*m/z* 1003.6 $[M+{}^{18}O_4+H]^+$)-containing peaks but was accompanied by significant peptide hydrolysis (data not shown). In light of this result, the doubly exchanged $^{18}O_2$-containing peptide was therefore identified as the appropriate isotope for use as a labeled reference standard. The major criterion for a stable isotope-labeled reference is that it contains a sufficient mass shift from the native compound to enable accurate quantification of the resulting isotopic doublets during co-analysis of the labeled and unlabeled compounds in an unknown mixture. The exchange of two ^{18}O atoms provides a 4-Da increase in molecular weight which satisfies this requirement. As shown in Table 2, the optimal abundance of the doubly exchanged, $^{18}O_2$-containing MC-LR peptide occurred after 48 h in a 5% TFA/$H_2{}^{18}O$ (97 at.%) solution, or after 72 h in the 2.5% TFA/$H_2{}^{18}O$ (97 at.%) mixture. In both cases, the doubly exchanged peak was the major product, with minimal starting (i.e., unlabeled) peptide remaining, and with only minor byproducts detected upon LC-MS analysis. Thus, while both of these final products are suitable for use as an internal reference compound, the 5% TFA/$H_2{}^{18}O$ (97 at.%) solution was chosen as the preferred exchange mixture due to the faster reaction time.

Treatment of the four commercially available MC-LR, MC-YR, MC-RR, and MC-LA variants with a 5% TFA/$H_2{}^{18}O$ (97 at.%) solution for 48 h (Table 3) gave similar ^{18}O-exchange levels to that observed for MC-LR. While only minor differences were seen in the isotopic distributions of MC-YR and MC-LA, which showed slight increases in the $^{18}O_3$-exchanged isotope, the doubly exchanged isotope was the dominant product in all cases along with near-complete consumption of the starting material. The propensity for $^{18}O \rightarrow {}^{16}O$ back exchange in each MC variant was then examined by dissolution of dried aliquots of the ^{18}O-exchanged peptides in 2% MeCN/0.1% formic acid (pH 2.1) for 24 h. Notably, no significant change in relative isotopic intensity of the $^{18}O_2$-containing signal was observed (Table 3), demonstrating that back-exchange does not occur under these conditions (i.e., exceeding the conditions to which the reference compounds would be exposed during sample preparation and analysis when used as internal standards), and therefore would not potentially

Table 2. Optimization of ^{18}O-exchange reaction conditions for microcystin-LR

^{18}O-exchange solvent composition	Reaction time (h)	Isotopic intensity (% total)				
		0 × ^{18}O	1 × ^{18}O	2 × ^{18}O	3 × ^{18}O	4 × ^{18}O
2.5% TFA/$H_2{}^{18}O$ (97 at.%)	24	6.9	34.5	46.7	10.9	1.0
	48	1.6	18.6	59.8	17.7	2.2
	72	0.6	11.6	60.9	23.3	3.7
	96	0.5	10.5	55.8	27.9	5.3
5.0% TFA/$H_2{}^{18}O$ (97 at.%)	24	1.7	18.8	57.7	19.5	2.3
	48	0.6	11.4	58.0	25.5	4.5
	72	0.5	10.2	51.7	30.6	7.0
	96	0.5	9.5	43.7	36.1	10.1

Table 3. ^{18}O-incorporation into microcystin-YR, microcystin-RR, and microcystin-LA peptides and monitoring of post-reaction back-exchange with ^{16}O

Solvent composition	Microcystin variant	Isotopic intensity (% total)				
		0 × ^{18}O	1 × ^{18}O	2 × ^{18}O	3 × ^{18}O	4 × ^{18}O
5.0% TFA/$H_2{}^{18}O$ (97 at.%)—48 h exchange reaction	MC-YR	1.2	7.5	47.5	35.0	8.8
	MC-RR	0.8	12.8	57.7	24.8	3.9
	MC-LA	0.1	6.2	51.5	34.3	7.9
2.0% MeCN/0.1% formic acid—24 h post-exchange reaction	MC-LR	1.0	10.6	55.7	27.7	5.0
	MC-YR	1.3	9.6	47.6	32.5	9.0
	MC-RR	0.9	13.9	57.0	24.3	3.9
	MC-LA	0.6	10.8	50.0	31.6	7.0

contribute to over-estimation of endogenous MCs. These results are consistent with literature accounts that describe similar observations of ^{18}O-labeled peptide stability in either 0.1 or 5% formic acid solutions [51–53].

Characterization of the $^{18}O_2$-containing product ions in each MC peptide by HCD-MS/MS revealed a 4-Da increase in all D-Glu (residue 6)-containing products, but surprisingly no increase in product ions containing D-MeAsp (residue 3) in the absence of D-Glu (Figure 6). Intramolecular bonding between Arg4 and MeAsp3 was eliminated as a possible reason for the MeAsp resistance to ^{18}O exchange, since the Arg-deficient, MC-LA showed the same bias toward the D-Glu-directed exchange (data not shown). Although substrate-dependent exchange rates have been reported for peptides in general [53], this unexpected result greatly simplifies the resultant fragmentation, allowing well-defined characterization of each MC variant based on their $^{18}O_2$-containing isotope containing product ions. The availability of stable isotope-containing MCs therefore enables their direct addition as internal standards into biological fluids, avoiding the requirement for labor-intensive, matrix-corrected solvent calibration [54]. Furthermore, the generation of any ^{18}O-labeled MC variant requires only the propagation and harvest of the cyanobacteria responsible, from which the required MC can be isolated. In unusual cases such as MCs that contain an esterified D-Glu residue, preclusion of the ^{18}O-exchange method is not critical from a health perspective since such glutamyl variations display very low toxicities [29] such that the detection of these peptides represents a much lower medical priority.

Detection and Absolute Quantitation of Microcystin-LR in Human Urine

Following characterization of the MS/MS fragmentation behavior of the MC-LR, MC-YR, MC-RR, and MC-LA peptides, only the accurate *m/z* values of the precursor ion, the global identifying ADDA fragment and the variant-specific product ion(s) of highest absolute abundance (using the optimized HCD (or UVPD)-MS/MS NCE values for each ion) are required for identification of these congeners at low concentrations in unknown mixtures. While the detection of multiple transitions is not required, additional fragments may be used to enhance identification specificity in mixtures of higher concentrations as their abundances become

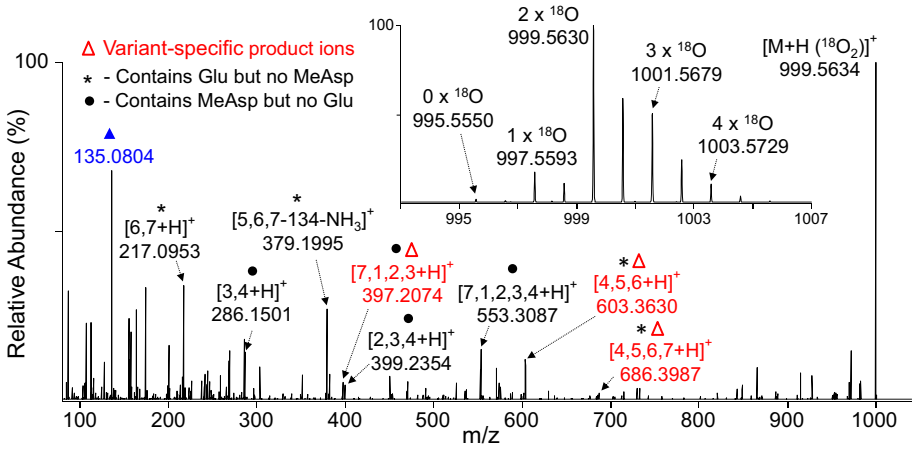

Figure 6. Representative HCD-MS/MS spectrum of the $[M+H]^+$ ion of $^{18}O_2$-stable isotope-labeled microcystin-LR (32% NCE). The isotopic distribution of the precursor ion from the MS spectrum is shown in the inset. The global microcystin-specific product ion is indicated by ▲; variant-specific product ions are indicated by empty red triangles. Product ions containing D-Glu but not D-MeAsp are indicated by an asterisk; product ions containing D-MeAsp but not D-Glu are indicated by △

greater than their respective limits of detection. In addition to the targeted identification of the four major MC congeners, this approach also allows the identification of unknown variants since the masses of structurally characteristic product ions formed from MC variants containing subtle structural variations may be readily predicted by comparison with the established fragmentation spectra from the current study. Importantly, various changes to the MC structure, such as amino acid residue substitutions in more conserved regions, or a methylated/demethylated variant(s), will not dramatically change the general fragmentation pattern, as suggested by the similar features of the MC-LR, MC-YR, MC-RR, and MC-LA product ion spectra. For example, HCD-MS/MS identification of a desmethyl-MC-LR variant, which lacks the methyl group attached to the β-carbon of the D-MeAsp residue at position 3, would proceed via initial assignment of the global ADDA fragment ion at *m/z* 135.08, along with observation of $[3,4+H]^+$ and isomer-specific $[7,1,2,3+H]^+$ product ions that also reflect the loss of the methyl group. Since only residue 3 is common to each of these fragments, the de-methylated modification could be isolated to this location, thereby providing the exact identity of the unknown MC variant. This approach may also be applied to the elucidation of primary sequence variations in the more conserved regions of the MC structure not only via the observation of isomer-specific product ions but also by accurate mass assignment of abundant non-specific products such as the $[6,7+H]^+$, $[7,1+H]^+$, $[7,1,2,3,4+H]^+$, and $[5,6,7\text{-}134\text{-}NH_3]^+$ product ions (Figure 2).

With regard to the detection of microcystins at low concentrations, the World Health Organization (WHO) has recommended a provisional guideline value of 1 μg/L for MC-LR (free plus cell-bound) in drinking water, with a fraction of the unbound toxin accumulating in urine, as demonstrated by earlier work in mice [31]. In cases where the urinary MC levels approach the limits of detection, it is anticipated that the high sensitivity of the ADDA product ion at *m/z* 135.08 from the doubly charged MC-LR, MC-YR, and MC-RR precursors will be the transition of highest analytical value, along with the mass and chromatographic retention time of the intact precursor. From a medical perspective, these MC concentrations would undoubtedly be asymptomatic. However, the significance of the more structurally informative variant-specific product ions would become apparent at higher concentrations.

To demonstrate the identification of MC peptides at relevant concentrations in human biofluids such as urine, a urine sample from a healthy subject was spiked with MC-LR at 1 μg/L then processed according to the simple general methodology outlined in Figure 7a (also see "Materials and Methods"), involving initial filtration using a low molecular weight cut-off filter followed by solid-phase extraction of the protein filtrate prior to LC-MS and targeted PRM-MS/MS analysis of the doubly charged MC-LR peptide. As shown in Figure 7b, chromatographic separation of the isolated protein mixture (corresponding to only 0.4 μL of the original urine sample; i.e., 400 fg of MC-LR) resulted in a large matrix background of other endogenous urinary peptides. However, PRM-MS/MS followed by extraction of the signal for the global ADDA-specific product ion (transition from *m/z* 498.3 → *m/z* 135.1) readily identified the MC-LR peptide at the expected elution time (21.2 min), with good signal-to-noise (Figure 7c). By

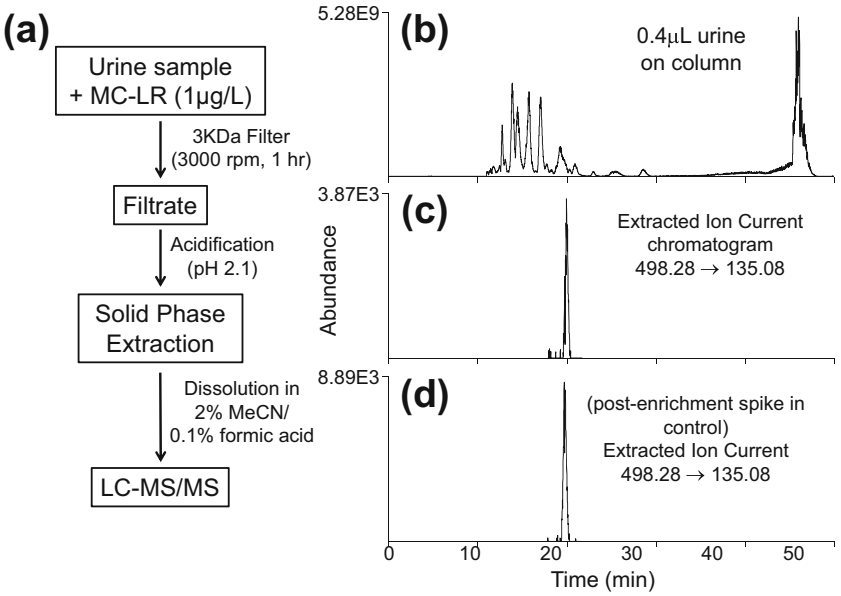

Figure 7. Quantitative analysis of microcystin-LR spiked into urine. (**a**) Schematic overview of the enrichment method. (**b**) LC-MS profile of the enriched low molecular weight peptide urine component, (**c**) extracted ion chromatogram of the global microcystin-specific ADDA product ion at *m/z* 135.08 from the $[M+2H]^{2+}$ precursor ion, and (**d**) extracted ion chromatogram of the global microcystin-specific ADDA product ion at *m/z* 135.08 from the $[M+2H]^{2+}$ precursor ion from a post-enrichment spike in control experiment

comparison of the abundance of this transition with that obtained from a post-enrichment spike in control experiment of MC-LR (also at 1 μg/L urine) (Figure 7d), the overall enrichment efficiency for the method was determined to be 43.5%. Although no other variant-specific ions were detected in the sample at this concentration, the results indicate that the general method developed and employed here provides a valid basis for the analysis of free microcystins in human urine at concentrations relevant to current guidelines. Furthermore, although not performed here, the utility of the ^{18}O-labeled reference materials will be demonstrated in future studies when appropriate contaminated samples of human biofluids such as urine containing endogenous MC are made available.

Pharmacokinetic studies have demonstrated considerable hepatic retention [55] and conjugation of MC peptides to cysteine-containing proteins such as glutathione [56] which indicates that initial ingestion of free MC is likely to provide a reduced fraction of unbound MC in the resulting urine. While the current study has focused on detection of free MC, an extension to this approach that would also enable the detection of bioconjugated MC could be achieved by the inclusion of an enzymatic digestion step prior to filtration. Through the judicious use of specific proteases that preclude MC digestion, the resulting microcystins that are bound to short, cleaved peptides would be liberated, albeit along with a large array of extraneous proteolytically derived peptides from the endogenous proteins. If this increase in peptide complexity was found to result in loss of MC detection/quantitation specificity during PRM-MS/MS, the addition of an immunoaffinity enrichment step, specific to the ADDA functionality, could be used to improve target peptide enrichment prior to solid phase extraction and subsequent LC-MS analysis.

Conclusions

By evaluating the use of various ion activation techniques including HCD-MS/MS, CID-MS/MS and MS^3, and 193 nm UVPD MS/MS, the global and variant-specific product ions for the identification, structural characterization, and absolute quantification of several representative MC peptides have been determined. In particular, the variables that give rise to structurally specific HCD-MS/MS and UVPD-MS/MS product ions have been optimized to provide the greatest instrumental detection sensitivity, critical for the determination of endogenous MC peptides in contaminated biological fluids. Using the methodologies described herein, the identification of a range of MC structural variants and their biotransformed (conjugated) products can be achieved via simple extrapolation of the MS/MS data based on the structural composition of the optimized fragmentation spectra. The absolute quantification of microcystins in contaminated urine samples has been addressed by the simple acid-catalyzed generation of stable $^{18}O_2$-containing MC peptides which provide a sufficient mass shift from the corresponding native peptides and without detrimental back-exchange, enabling their use as internal standards. Finally, the analysis methods described herein have been applied toward the identification of the common MC-LR peptide in human urine, at concentrations relevant to WHO provisional guidelines. Based on these results, we anticipate that the analytical methodologies outlined in this study will contribute to the development of improved procedures for the prompt identification of ingested MC toxins and will have utility for expedited diagnosis and medical treatment.

Disclaimer

The findings and conclusions in this study are those of the authors and do not necessarily represent the views of the US Department of Health and Human Services or the US Centers for Disease Control and Prevention. Use of trade names and commercial sources is for identification only and does not constitute endorsement by the US Department of Health and Human Services or the US Centers for Disease Control and Prevention.

Funding Information

Financial support for this work was received under contract 200-2014-59255 from The Centers for Disease Control and Prevention (CDC), National Center for Environmental Health (NCEH), Division of Laboratory Sciences (DLS), Emergency Response Branch (ERB), Atlanta, Georgia, USA.

References

1. Zurawell, R.W., Chen, H., Burke, J.M., Prepas, E.E.: Hepatotoxic cyanobacteria: a review of the biological importance of microcystins in freshwater environments. J. Toxicol. Environ. Health B Crit. Rev. **8**, 1–37 (2005)
2. Vasconcelos, J.F., Barbosa, J.E.L., Lira, W., Azevedo, S.M.F.O.: Microcystin bioaccumulation can cause potential mutagenic effects in farm fish. Egypt. J. Aquat. Res. **39**, 185–192 (2013)
3. Pavagadhia, S., Balasubramanian, R.: Toxicological evaluation of microcystins in aquatic fish species: current knowledge and future directions. Aquat. Toxicol. **142–143**, 1–16 (2013)
4. DeVries, S.E., Galey, F.D., Namikoshi, M., Woo, J.C.: Clinical and pathologic findings of blue-green algae (Microcystis aeruginosa) intoxication in a dog. J. Vet. Diagn. Investig. **5**, 403–408 (1993)
5. Briand, J.-F., Jacquet, S., Bernard, C., Humbert, J.-F.: Health hazards for terrestrial vertebrates from toxic cyanobacteria in surface water ecosystems. Vet. Res. **34**, 361–377 (2003)
6. Gilroy, D.J., Kauffman, K.W., Hall, R.A., Huang, X., Chu, F.S.: Assessing potential health risks from microcystin toxins in blue-green algae dietary supplements. Environ. Health Perspect. **108**, 435–439 (2000)
7. Vichi, S., Lavorini, P., Funari, E., Scardala, S., Testai, E.: Contamination by Microcystis and microcystins of blue-green algae food supplements (BGAS) on the Italian market and possible risk for the exposed population. Food Chem. Toxicol. **50**, 4493–4499 (2012)
8. Herranz, S., Bocková, M., Marazuela, M.D., Homola, J., Moreno-Bondi, M.C.: An SPR biosensor for the detection of microcystins in drinking water. Anal. Bioanal. Chem. **398**, 2625–2634 (2010)
9. Cook, D., Newcombe, G.: Comparison and modeling of the adsorption of two microcystin analogues onto powdered activated carbon. Environ. Technol. **29**, 525–534 (2008)
10. Yu, S.-Z.: Primary prevention of hepatocellular carcinoma. J. Gastroenterol. Hepatol. **10**, 674–682 (1995)
11. Ueno, Y., Nagata, S., Tsutsumi, T., Hasegawa, A., Watanabe, M.-F., Park, H.-D., Chen, G.-C., Chen, G., Yus, S.-Z.: Detection of microcystins, a blue-green algal hepatotoxin, in drinking water sampled in Haimen and Fusui, endemic areas of primary liver cancer in China, by highly sensitive immunoassay. Carcinogenesis. **17**, 1317–1321 (1996)

12. Svirčev, Z., Krstić, S., Miladinov-Mikov, M., Baltić, V., Vidović, M.: Freshwater cyanobacterial blooms and primary liver cancer epidemiological studies in Serbia. J. Environ. Sci. Health Part C. **27**, 36–55 (2009)
13. Diehnelt, C.W., Peterman, S.M., Budde, W.L.: Liquid chromatography–tandem mass spectrometry and accurate *m/z* measurements of cyclic peptide cyanobacteria toxins. Trends Anal. Chem. **24**, 622–634 (2005)
14. Khreich, N., Lamourette, P., Renard, P.-Y., Clavé, G., Fenaille, F., Créminon, C., Volland, H.: A highly sensitive competitive enzyme immunoassay of broad specificity quantifying microcystins and nodularins in water samples. Toxicon. **53**, 551–559 (2009)
15. de Silva, E.D., Williams, D.E., Andersen, R.J.: Motuporin, a potent protein phosphatase inhibitor isolated from the Papua New Guinea sponge Theonella swinhoei Gray. Tet. Lett. **33**, 1561–1564 (1992)
16. Hotto, A.M., Satchwell, M.F., Berry, D.L., Gobler, C.J., Boyer, G.L.: Spatial and temporal diversity of microcystins and microcystin-producing genotypes in Oneida Lake, NY. Harmful Algae. **7**, 671–681 (2008)
17. Namikoshi, M., Rinehart, K.L., Sakai, R.: Identification of 12 hepatotoxins from a Homer Lake bloom of the cyanobacteria Microcystis aeruginosa, Microcystis viridis, and Microcystis wesenbergii: nine new microcystins. J. Org. Chem. **57**, 866–872 (1992)
18. Namikoshi, M., Rinehart, K.L., Sakai, R.: Structures of three new cyclic heptapeptide hepatotoxins produced by the cyanobacterium (blue-green alga) Nostoc sp. strain 152. J. Org. Chem. **55**, 6135–6139, 1990
19. Harada, K., Ogawa, K., Matsuura, K., Murata, H., Suzuki, M.: Structural determination of geometrical isomers of microcystins LR and RR from cyanobacteria by two-dimensional NMR spectroscopic techniques. Chem. Res. Toxicol. **3**, 473–481 (1990)
20. Puerto, M., Pichardo, S., Jos, A., Camean, A.M.: Comparison of the toxicity induced by microcystin-RR and microcystin-YR in differentiated and undifferentiated Caco-2 cells. Toxicon. **54**, 161–169 (2009)
21. Namikoshi, M., Choi, B.W., Sun, F., Rinehart, K.L., Evans, W.R., Carmichael, W.W.: Chemical characterization and toxicity of dihydro derivatives of nodularin and microcystin-LR, potent cyanobacterial cyclic peptide hepatotoxins. Chem. Res. Toxicol. **6**, 151–158 (1993)
22. Namikoshi, M., Sun, F., Choi, B.W., Rinehart, K.L., Carmichael, W.W., Evans, W.R.: Seven more microcystins from Homer Lake cells: application of the general method for structure assignment of peptides containing alpha-, beta-dehydroamino acid unit(s). J. Org. Chem. **60**, 3671–3679 (1995)
23. Harada, K., Ogawa, K., Kimura, Y., Murata, H., Suzuki, M., Thorn, P.M., Evans, W.R., Carmichael, W.W.: Microcystins from Anabaena flos-aquae NRC 525-17. Chem. Res. Toxicol. **4**, 535–540 (1991)
24. Stotts, R.R., Namikoshi, M., Haschek, W.M., Rinehart, K.L., Carmichael, W.W., Dahlem, A.M., Beasley, V.R.: Structural modifications imparting reduced toxicity in microcystins from Microcystis spp. Toxicon. **31**, 783–789 (1993)
25. Sherlock, I.R., James, K.J., Caudwell, F.B., MacKintosh, C.: First identification of microcystins in Irish lakes aided by a new derivatisation procedure for electrospray mass spectrometric analysis. Nat. Toxins. **5**, 247–254 (1997)
26. Geis-Asteggiante, L., Lehotay, S.J., Fortis, L.L., Paoli, G., Wijey, C., Heinzen, H.: Development and validation of a rapid method for microcystins in fish and comparing LC-MS/MS results with ELISA. Anal. Bioanal. Chem. **401**, 2617–2630 (2011)
27. Yuan, M., Namikoshi, M., Otsuki, A., Rinehart, K.L., Sivonen, K., Watanabe, M.F.: Low-energy collisionally activated decomposition and structural characterization of cyclic heptapeptide microcystins by electrospray ionization mass spectrometry. J. Mass Spectrom. **34**, 33–34 (1999)
28. Mayumi, T., Kato, H., Imanishi, S., Kawasaki, Y., Hasegawa, M., Harada, K.: Structural characterization of microcystins by LC/MS/MS under ion trap conditions. J. Antibiot. **59**, 710–719 (2006)
29. Frias, H.V., Mendes, M.A., Cardozo, K.H.M., Carvalho, V.M., Tomazela, D., Colepicolo, P., Pinto, E.: Use of electrospray tandem mass spectrometry for identification of microcystins during a cyanobacterial bloom event. Biochem. Bioph. Res. Co. **344**, 741–746 (2006)
30. de Graaf, E.L., Altelaar, A.F.M., van Breukelen, B., Mohammed, S., Heck, A.J.R.: Improving SRM assay development: a global comparison between triple quadrupole, ion trap, and higher energy CID peptide fragmentation spectra. J. Proteome Res. **10**, 4334–4341 (2011)
31. Brodbelt, J.S.: Ion activation methods for peptides and proteins. Anal. Chem. **88**, 30–51 (2016)
32. Brodbelt, J.S.: Photodissociation mass spectrometry: new tools for characterization of biological molecules. Chem. Soc. Rev. **43**, 2757–2783 (2014)
33. Theisen, A., Yan, B., Brown, J.M., Morris, M., Bellina, B., Barran, P.E.: Use of ultraviolet photodissociation coupled with ion mobility mass spectrometry to determine structure and sequence from drift time selected peptides and proteins. Anal. Chem. **88**, 9964–9971 (2016)
34. Madsen, J.A., Boutz, D.R., Brodbelt, J.S.: Ultrafast ultraviolet photodissociation at 193 nm and its applicability to proteomic workflows. J. Prot. Res. **9**, 4205–4214 (2010)
35. Fort, K.L., Dyachenko, A., Potel, C.M., Corradini, E., Marino, F., Barendregt, A., Makarov, A.A., Scheltema, R.A., Heck, A.J.R.: Implementation of ultraviolet photodissociation on a benchtop Q exactive mass spectrometer and its application to phosphoproteomics. Anal. Chem. **88**, 2303–2310 (2016)
36. Cleland, T.P., DeHart, C.J., Fellers, R.T., VanNispen, A.J., Greer, J.B., LeDuc, R.D., Parker, W.R., Thomas, P.M., Kelleher, N.L., Brodbelt, J.S.: High-throughput analysis of intact human proteins using UVPD and HCD on an Orbitrap mass spectrometer. J. Prot. Res. **16**, 2072–2079 (2017)
37. O'Brien, J.P., Li, W., Zhang, Y., Brodbelt, J.S.: Characterization of native protein complexes using ultraviolet photodissociation mass spectrometry. J. Am. Chem. Soc. **136**, 12920–12908 (2014)
38. Mistarz, U.H., Bellina, B., Jensen, P.F., Brown, J.M., Barran, P.E., Rand, K.D.: UV Photodissociation mass spectrometry accurately localize sites of backbone deuteration in peptides. Anal. Chem. **90**, 1077–1080 (2018)
39. Crittenden, C.M., Parker, W.R., Jenner, Z.B., Bruns, K.A., Akin, L.D., McGee, W.M., Ciccimaro, E., Brodbelt, J.S.: Exploitation of the ornithine effect enhances characterization of stapled and cyclic peptides. J. Am. Soc. Mass Spectrom. **27**(5), 856–863 (2016)
40. Ozawa, K.; Fujioka, H.; Muranaka, M.; Yokoyama, A.; Katagami, Y.; Homma, T.; Ishikawa, K.; Tsujimura, S.; Kumagai, M.; Watanabe, M.F.; Park, H-D. Spatial distribution and temporal variation of Microcystis species composition and microcystin concentration in Lake Biwa. Environ. Toxicol. 20, 270–276 (2005)
41. Szlag, D.C., Sinclair, J.L., Southwell, B., Westrick, J.A.: Cyanobacteria and cyanotoxins occurrence and removal from five high-risk conventional treatment drinking water plants. Toxins. **7**, 2198–2220 (2015)
42. Flores, C., Caixach, J.: An integrated strategy for rapid and accurate determination of free and cell-bound microcystins and related peptides in natural blooms by liquid chromatography-electrospray-high resolution mass spectrometry and matrix-assisted laser desorption/ionization time-of-flight/time-of-flight mass spectrometry using both positive and negative ionization modes. J. Chromatogr. A. **1407**, 76–89 (2015)
43. Ryan, E., Nguyen, C.Q.N., Shiea, C., Reid, G.E.: Detailed structural characterization of sphingolipids via 193 nm ultraviolet Photodissociation and ultra high resolution tandem mass spectrometry. J. Am. Soc. Mass Spectrom. **28**, 1406–1419 (2017)
44. Miles, C.O., Sandvik, M., Nonga, H.E., Rundberget, T., Wilkins, A.L., Rise, F., Ballot, F.: Identification of microcystins in a Lake Victoria cyanobacterial bloom using LC-MS with thiol derivatization. Toxicon. **70**, 21–31 (2013)
45. Boyd, R., Somogy, Á.: The mobile proton hypothesis in fragmentation of protonated peptides: a perspective. J. Am. Soc. Mass Spectrom. **21**, 1275–1278 (2010)
46. Grach-Pogrebinsky, O., Sedmak, B., Carmeli, S.: Seco[D-Asp3]microcystin-RR and [D-Asp3,D-Glu(OMe)6]microcystin-RR, two new microcystins from a toxic water bloom of the cyanobacterium planktothrixrubescens. J. Nat. Prod. **67**, 337–342 (2004)
47. Brittain, S., Mohamed, S.A., Wang, J., Lehmann, V.K.B., Carmichael, W.W., Rinehart, K.L.: Isolation and characterization of microcystins from a River Nile strain of Oscillatoria tenuis Agardh ex Gomont. Toxicon. **38**, 1759–1771 (2000)
48. Pearson, C., Rinehart, K.L., Sugano, M., Costerison, J.R.: Enantiospecific synthesis of N-BOC-ADDA: a linear approach. Org. Lett. **2**, 2901–2903 (2000)
49. Clavé, G., Ronco, C., Boutal, H., Kreich, N., Volland, H., Franck, X., Romieu, A., Renard, P.-Y.: Facile and rapid access to linear and truncated microcystin analogues for the implementation of immunoassays. Org. Biomol. Chem. **8**, 676–690 (2010)
50. Naidu, B.N., Sorenson, M.E., Connolly, T.P., Ueda, Y.: Michael addition of amines and thiols to dehydroalanine amides: a remarkable rate acceleration in water. J. Org. Chem. **68**, 10098–10102 (2003)
51. Haaf, E., Schlosser, A.: Peptide and protein quantitation by acid-catalyzed 18O-labeling of carboxyl groups. Anal. Chem. **84**, 304–311 (2012)

52. Niles, R., Witkowska, H.E., Allen, S., Hall, S.C., Fisher, S.J., Hardt, M.: Acid-catalyzed oxygen-18 labeling of peptides. Anal. Chem. **81**, 2804–2809 (2009)
53. Liu, N., Wu, H., Liu, H., Chen, G., Cai, Z.: Microwave-assisted 18O-labeling of proteins catalyzed by formic acid. Anal. Chem. **82**, 9122–9126 (2010)
54. Parker, C.H., Stutts, W.L., DeGrasse, S.L.: Development and validation of a liquid chromatography-tandem mass spectrometry method for the quantitation of microcystins in blue-green algal dietary supplements. J. Agric. Food Chem. **63**, 10303–10312 (2015)
55. Robinson, N.A., Pace, J.G., Matson, C.F., Miura, G.A., Lawrence, W.B.: Tissue distribution, excretion and hepatic biotransformation of microcystin-LR in mice. J. Pharmacol. Exp. Therapeutics. **256**, 176–182 (1991)
56. Buratti, F.M., Testai, E.: Species- and congener-differences in microcystin-LR and -RR GSH conjugation in human, rat, and mouse hepatic cytosol. Toxicol. Lett. **232**, 133–140 (2015)